Diffuse Reflectance Spectra of Al Substituted Goethite: A Ligand Field Approach

Article *in* Clays and Clay Minerals · April 1999

DOI: 10.1346/CCMN.1999.0470205

CITATIONS
62

READS
218

3 authors, including:

Andreas C Scheinost
Helmholtz-Zentrum Dresden-Rossendorf
278 PUBLICATIONS **8,175** CITATIONS
SEE PROFILE

Darrell Schulze
Purdue University
88 PUBLICATIONS **3,644** CITATIONS
SEE PROFILE

Clays and Clay Minerals, Vol. 47, No. 2, 156–164, 1999.

DIFFUSE REFLECTANCE SPECTRA OF Al SUBSTITUTED GOETHITE: A LIGAND FIELD APPROACH

ANDREAS C. SCHEINOST,[1†] DARRELL G. SCHULZE,[1] AND UDO SCHWERTMANN[2]

[1] Agronomy Department, Purdue University, West Lafayette, Indiana 47907
[2] Lehrstuhl Für Bodenkunde, TU München, 85350 Freising, F.R.G.

Abstract—Previous investigations of goethite revealed a substantial variation of color and diffuse reflectance spectra (DRS) in the extended visible range (350–2200 nm). To better understand the causes of this variability and to assess the potential of DRS as a mineralogical tool, we investigated the DRS of pure and Al-substituted goethite, α-$Fe_{1-x}Al_xOOH$ with x from 0 to 0.33, and mean crystal lengths (MCL) from 170 to 1800 nm. The strongly overlapping ligand field bands were extracted by fitting the single-electron transitions $^6A_1 \rightarrow {}^4T_1$, $^6A_1 \rightarrow {}^4T_2$, $^6A_1 \rightarrow ({}^4E; {}^4A_1)$, and $^6A_1 \rightarrow {}^4E({}^4D)$ as functions of the ligand field splitting energy, 10 Dq, and the interelectronic repulsion parameters, Racah-B and -C. With x increasing from 0 to 0.33, $^6A_1 \rightarrow {}^4T_1$ decreased from 10,590 to 10,150 cm^{-1} (944 to 958 nm), and $^6A_1 \rightarrow {}^4T_2$ decreased from 15,310 to 14,880 cm^{-1} (653 to 672 nm), while 10 Dq increased from 15,770 to 16,220 cm^{-1}. From the change of 10 Dq we calculated a decrease of the Fe-(O,OH) distances from 202.0 to 200.9 pm (−0.5%). This decrease is smaller than the average decrease of all (Al,Fe)-(O,OH) distances (−1.8%) calculated from the change of the unit-cell lengths (UCL). That is, there remains a substantial difference in size between the larger Fe- and the smaller Al-occupied octahedra in the solid solution which may indicate the existence of diaspore clusters within the goethite structure. The increasing strain in the crystal structure due to the size mismatch and limited contractibility of the oxygen cage around Fe may be the primary reason for Al substitution being restricted to $x < 0.33$. The bands $^6A_1 \rightarrow ({}^4E; {}^4A_1)$ and $^6A_1 \rightarrow {}^4E({}^4D)$ did not shift, indicating a constant covalency of the Fe-(O,OH) bonds with B = 628 cm^{-1} and $C = 5.5B$. Whereas variation of band energies could be explained in terms of the Fe-(O,OH) ligand field, the variation of color and band intensities was mainly determined by crystal size. Although our study confirmed the potential of DRS for mineralogical investigations, there is still a gap between the fundamental theory and the explanation of some spectral features.

Key Words—Band Decomposition, Bond Distances, Diffuse Reflectance Spectroscopy, Goethite, Ligand Field Splitting, Racah-Parameters.

INTRODUCTION

Iron (hydr)oxides show absorption bands at ultraviolet (UV) to near infrared (IR) wavelengths which are caused by electronic transitions within the incompletely filled, $3d^5$ shell of Fe(III) (Burns, 1993). The energy splitting within the 3d shell is created by the ligand field of six O or OH anions in octahedral symmetry. As the structures of all Fe (hydr)oxides are comprised of these $Fe(O,OH)_6$ octahedra, their spectra show the same bands. Differences between the spectra of iron oxide minerals occur, however, because of the different linkages of the octahedra (Manceau and Combes, 1988). Distortions of the octahedra alter the Fe-(O,OH) distances and lower the symmetry, factors which in turn alter the ligand field and shift band positions (Burns, 1993). Differences in the Fe-to-Fe distances, on the other hand, have an influence on the magnetic coupling of electron spins at neighboring Fe centers which may modify the intensity of bands (Sherman and Waite, 1985).

Because of the sensitivity to these differences, reflectance spectra were used to infer the Fe (hydr)oxide mineralogy of samples on very different scales, ranging from the remote sensing of the surfaces of Earth, Mars and other planets (Singer, 1982; Buckingham and Sommer, 1983; Morris *et al.*, 1997; Bishop and Murad, 1996) to occlusions in kaolinite particles (Malengreau *et al.*, 1994). Recent work showed, however, that the band positions vary substantially within minerals, leading to strongly overlapping band regions between the Fe (hydr)oxide minerals (Scheinost *et al.*, 1998). This study showed that most Fe (hydr)oxide minerals may be discriminated in monomineralic mixtures, but only hematite and magnetite can be unequivocally discriminated when soils contain several Fe (hydr)oxides.

The variability of band positions within Fe (hydr)oxide minerals, which often hinders the unique assignment of minerals from reflectance spectra, may reveal, on the other hand, useful information on the crystal structure. Buckingham and Sommer (1983) found that the $^6A_1 \rightarrow {}^4T_1$ transition of goethite, a clearly resolved band in the near IR, was shifted to lower energy when Al was incorporated in the goethite structure. They explained the shift by the decrease of the UCL towards that of the pure Al end-member diaspore, and a subsequent decrease of the Fe-(O,OH) distances which, in turn, would increase 10 Dq. Morris

† Present address: Department of Plant and Soil Sciences, University of Delaware, Newark, Delaware 19717-1303

Table 1. Synthesis procedures and extent of Al substitution of the goethite series.

Series	Source of Fe and Al	Base	T/°C	Time/d	x/mol mol^{-1}
28	$Fe(NO_3)_3$, $Al(NO_3)_3$	0.35–0.40 M KOH	70	14	0–0.17
31	$Fe(NO_3)_3$, $Al(NO_3)_3$	0.3 M KOH	70	14	0–0.10
34	$Fe(NO_3)_3$, $AlCl_3$	0.3 M KOH	70	14	0–0.08
35	$Fe(NO_3)_3$, $AlCl_3$	0.3 M KOH	25	1310	0–0.17
38	$FeCl_3$, $AlCl_3$	0.3 M KOH	25	1310	0.33
53	$Fe(NO_3)_3$, $AlCl_3$	0.3 M KOH	50	44	0–0.13
58	$Fe(NO_3)_3$, $AlCl_3$	0.3 M KOH	35	459	0–0.12
39	$Fe(NO_3)_3$	0.7 M KOH	4–70	6–68	0
54/0	$Fe(NO_3)_3$	0.3 M KOH	70	111	0

et al. (1992) confirmed this by a linear relation between $^6A_1 \rightarrow {}^4T_1$ and the inverse fifth-power of UCL_a of hematite. The intercepts and slopes of the regression equations varied, however, between different synthesis series.

Kosmas *et al.* (1986) found a blue shift of the main absorption edge in the visible region, determined by the second derivative minimum, when the Al substitution of synthetic goethite increased (r = 0.99). Despite this blue shift, the Munsell hue was shifted towards red (r = 0.82). From multiple regression analysis, they concluded that part of the red shift was caused by decreasing MCL. Malengreau *et al.* (1996) confirmed the blue shift of the main absorption edge, assigned to the electron pair transition (EPT), $(^6A_1 + {}^6A_1) \rightarrow ({}^4T_1 + {}^4T_1)$, but were not able to establish a quantitative relationship between band shift and x of natural goethite samples.

Thus, Al substitution was observed to shift the two main features of the goethite spectra, the absorption edge in the visible region, and the relatively isolated band in the near IR region. Experimental transmission spectra of hematite single crystals and thin films (Marusak *et al.,* 1980), ligand field calculations (Orgel, 1952; Lever, 1984), and molecular orbital calculations (Tossell and Vaughan, 1974; Sherman, 1985; Sherman and Waite, 1985) revealed, however, at least six 3d transitions between 250–950 nm, in addition to charge transfer bands in the UV (Burns, 1993). In contrast to transmission spectra of oriented crystals, DRS bands are broader due to random orientation of crystallographic axes and scattering effects of the powder samples, leading to strongly overlapping and merging bands. Derivative spectroscopy was, therefore, not suited for resolving the positions of more than three ligand-field bands in the UV-VIS region (Kosmas *et al.,* 1984; Malengreau *et al.,* 1994). The decomposition of the spectra by a nonlinear fit of Gaussian distributions may allow all bands to be determined (Sunshine *et al.,* 1990). A preliminary investigation showed, however, that several combinations of Gaussians produced similar fits of the spectra, *i.e.,* there was no unique solution. Therefore, the purpose of this study was (1) to achieve a more reliable decomposition by fitting band positions as functions of 10 Dq, Racah-*B,* and Racah-*C,* (2) to investigate the influence of Al substitution on band positions, (3) to infer the effect of Al substitution on the ligand field around Fe(III), and (4) to investigate whether the influence of Al substitution on the ligand field or particle size effects contribute to the observed color changes. Benefits of this research are expected to be two-fold, first, in providing a better understanding of the α-$Fe_{1-x}Al_xOOH$ structure, and second, in developing a better understanding of the variability of DRS of soils. Although our study included only synthetic goethites, the results should be applicable to spectra from soils because of the ubiquity of goethite and the widespread occurrence of Al substitution ($x \leq 0.20$) in this mineral (Fitzpatrick and Schwertmann, 1982; Carlson, 1995; Cornell and Schwertmann, 1996).

MATERIALS AND METHODS

Goethite samples

Goethites from seven synthesis series contained variable amounts of Al (determined wet-chemically) substituted in the goethite structure as verified by the decrease of UCL (Table 1). Data for series 28 and 31 are published in Schulze (1984), data for series 34 and 38 are in Schulze and Schwertmann (1984), and data for series 35 are in Schulze and Schwertmann (1987). Series 53 and 58 were synthesized similar to series 34 and 35 (Schwertmann and Craciun, unpublished). The samples cover the range of possible Al substitution with $0 \leq x \leq 0.33$. The unsubstituted series 39, synthesized at temperatures between 4–60°C (Schwertmann *et al.,* 1985), and sample 54/0 (Schwertmann *et al.,* 1989) provided MCLs between 170–1800 nm (Table 1). Thus, we were able to investigate crystal-size effects independently from Al substitution. The purity of all samples was checked with X-ray diffraction (XRD) and, with respect to hematite impurities, by more sensitive diffuse reflectance spectroscopy (Scheinost *et al.,* 1998). The MCLs were determined using a JEOL 2000 FX high resolution transmission electron microscope operated at 200 kV. Samples were ultrasonically dispersed in distilled water. A drop of the suspension

was placed on a carbon-coated copper grid and allowed to air dry. Magnification was adjusted between 12,000–120,000 depending on crystal size. Crystallographic *c*-dimensions of at least 50 crystals per sample were averaged to MCL.

Spectral measurements and color calculations

DRS were measured with a Lambda 19 spectrophotometer (Perkin Elmer) equipped with a Spectralon-coated integrating sphere 15 cm in diameter (Labsphere). Spectra were recorded from 300 to 2200 nm in 1 nm steps, with a scan speed of 240 nm min^{-1}. Absolute reflectance was calculated using a Spectralon standard with known reflectance. The undiluted powder samples were filled in Plexiglas holders 51 mm in diameter and 1 mm in depth and measured without cover glasses.

The visible portion of the spectra was used to calculate the X, Y, and Z tristimulus values (Wyszecki and Stiles, 1982). These were converted into polar coordinates of three color spaces: (1) hue, chroma, and value of the Munsell system (Fernandez and Schulze, 1987), (2) hue, chroma, and lightness (equivalent to value) of the CIE-L*a*b* system (Melville and Atkinson, 1985), and (3) the dominant wavelength (equivalent to hue), the excitation purity (equivalent to chroma), and the lightness of the basic, non-uniform chromaticity system (Bedidi *et al.*, 1992). Because the observed trends of color were identical in all three systems, results are shown for the Munsell system only.

Spectral decomposition

The DRS were decomposed using Gaussians

$$\log[R(E)] = \sum_{i=1}^{n} - h_i \times \exp\left[-\left(\frac{E - E_i}{FWHH_i}\right)^2 \times 4 \ln(2)\right] \quad (1)$$

where R is the reflectance; E is the energy in wavenumber [cm^{-1}], h_i is the height of the i^{th} absorption band, E_i is the mean energy [cm^{-1}] of the ith band, and $FWHH_i$ is the full width at half height of the ith band [cm^{-1}]. Log reflectance was chosen because of a narrower distribution of the band heights as compared to the Kubelka-Munk remission function. In the latter, the height of the lower-energy bands is drastically reduced because of the reciprocal relation between remission and reflectance. Thus, the squared-difference minimization procedure necessarily results in much less precise band estimates for the low-energy bands which are, however, critical for determining 10 Dq (see below). The best fit in terms of (1) the smallest deviation between the fitted and the measured spectra, (2) parameter estimates with the lowest asymptotic standard deviations, and (3) conclusiveness within the ligand field theory, was achieved with six Gaussians. The energies, E_i, of four sextet-quartet-transitions were fit as functions of 10 Dq, B and C (Lever, 1984):

$$\begin{aligned} E(^6A_1 \rightarrow {}^4T_1) &= -10\ Dq + 10B + 6C \\ &\quad -26B^2/10\ Dq \\ E(^6A_1 \rightarrow {}^4T_2) &= -10\ Dq + 18B + 6C \\ &\quad - 38B^2/10\ Dq \\ E(^6A_1 \rightarrow ({}^4E; {}^4A_1)) &= 10B + 5C \\ E(^6A_1 \rightarrow {}^4E({}^4D)) &= 17B + 5C. \end{aligned} \quad (2)$$

The decomposition was performed using the SAS command language and the Marquardt nonlinear regression method (SAS Institute Inc., 1988). The single electron transitions correspond with bands 1, 2, 5, and 6 in Figure 1. Two additional bands, 3 and 4, were necessary to fit the high step at ~19,000 cm^{-1}. They could not be assigned to any of the one-electron transitions. Both were within ±2000 cm^{-1} of $2 \times E(^6A_1 \rightarrow {}^4T_1)$, and therefore fulfilled the criterion for the EPT (Sherman and Waite, 1985). Because of the lack of ligand field equations for these two bands, their band energies were fit independently. When B and C of the single electron transitions were fit as free parameters, they were (1) highly correlated ($r > 0.99$) resulting in meaningless values, and (2) the small hump visible in the spectra of higher substituted goethites at the position of $^6A_1 \rightarrow ({}^4E;{}^4A_1)$ (~23,500 cm^{-1}, see Figure 1) was not properly fit. By an iterative-optimization procedure, we found that all spectra could be well described with fixed B = 628 cm^{-1} and $C = 5.5B$ = 3454 cm^{-1}. The remaining 15 parameters (10 Dq, energy of band 3 and 4, heights and widths of all bands) were fit without constraints using the spectral range from 8500 to 28,500 cm^{-1}.

RESULTS AND DISCUSSION

Influence of Al substitution on band positions and intensities

The reflectance spectra of the unsubstituted and the Al goethites are similar to those reported earlier (Sherman *et al.*, 1982; Singer, 1982; Townsend, 1987) with some obvious changes with increasing Al (Figure 2). The most significant is the shift of $^6A_1 \rightarrow {}^4T_1$ to lower energy which was observed earlier for goethite and for hematite (Buckingham and Sommer, 1983; Morris *et al.*, 1992). The $^6A_1 \rightarrow {}^4T_2$ and the EPT_1 bands increasingly overlap, and the EPT region changes from a rounded curve to a relatively straight step. The EPT region ends in a pronounced band at the lower end. Neither location nor intensity of the OH overtone and OH combination bands at energies lower than 8500 cm^{-1} changes markedly (OH in Figure 2).

For Al-substituted hematite, Morris *et al.* (1992) deduced the shift of $^6A_1 \rightarrow {}^4T_1$ from an increase of 10

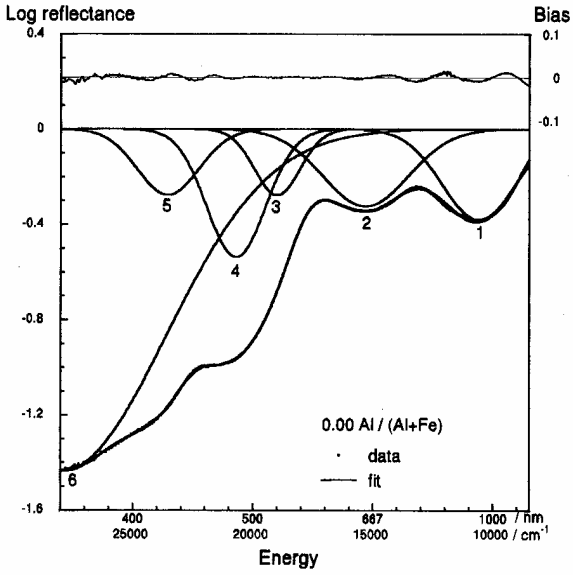

Figure 1. Decomposition of the absorption bands of pure goethite (top) and of Al substituted goethite (x_r = 0.33, bottom).

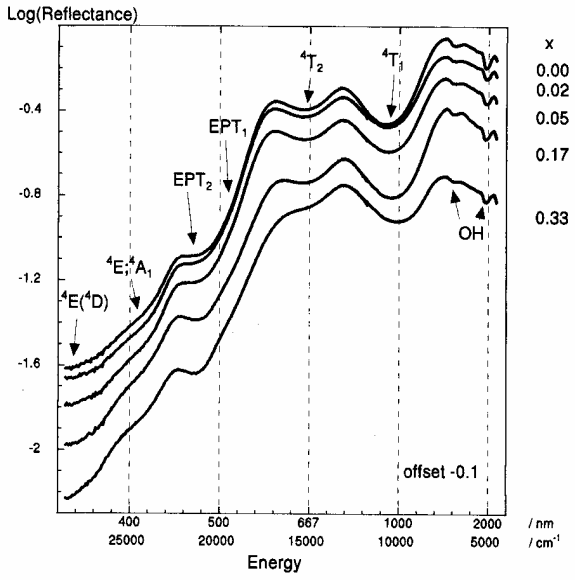

Figure 2. DRS of goethite with increasing Al substitution (series 35 and 38). Successive spectra are shifted downward by 0.1. Arrows show the position of bands which have been used for the decomposition of the spectra, except for the OH overtone and combination bands (OH).

Dq. According to Equation (2), however, not only $^6A_1 \rightarrow {}^4T_1$, but also $^6A_1 \rightarrow {}^4T_2$ should decrease with increasing 10 Dq. The band positions of $^6A_1 \rightarrow {}^4T_1$ and $^6A_1 \rightarrow {}^4T_2$, as determined by the decomposition method described above, support this conclusion (Figure 3). Independent of the synthesis conditions, $^6A_1 \rightarrow {}^4T_1$ linearly decreases from 10,590 to 10,150 cm^{-1} (944 to 958 nm), and $^6A_1 \rightarrow {}^4T_2$ decreases from 15,310 to 14,880 cm^{-1} (653 to 672 nm) when x increases from 0 to 0.33. Consequently, 10 Dq increases linearly from 15,770 to 16,220 cm^{-1} with increasing x (Figure 4, top). A similar relation between 10 Dq and x could be established for the nearly complete solid-solution series of $Cr_xAl_{2-x}O_3$ (Reinen, 1969), confirming the earlier prediction of Orgel (1957) that the introduction of the larger Cr ion would lead to site compression around Cr rather than to relaxation of the host lattice.

It is well known that the smaller ionic radius of Al(III) (53.5 pm as compared to 64.5 pm of Fe(III); Shannon, 1976) reduces the lattice of Al-substituted goethite (Schulze, 1984; Wolska and Schwertmann, 1993; Schwertmann and Carlson, 1994). Accordingly, the UCLs (in nm) along the crystallographic axes *a, b* and *c* decrease:

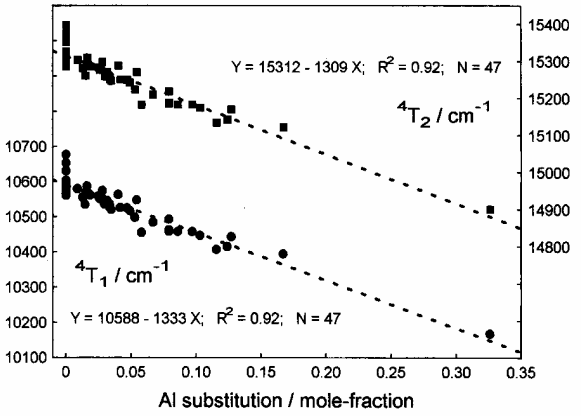

Figure 3. Band shifts of the lowest transitions $^6A_1 \rightarrow {}^4T_1$ and $^6A_1 \rightarrow {}^4T_2$ with increasing Al substitution.

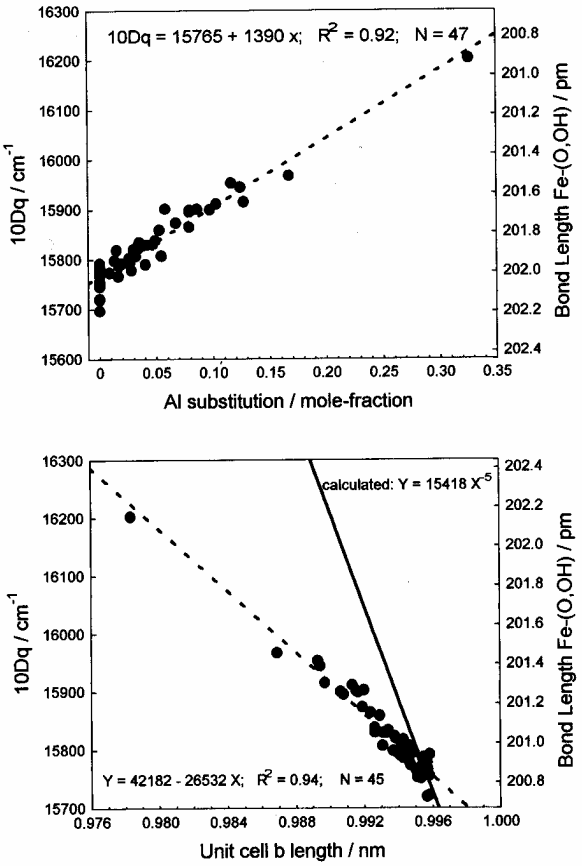

Figure 4. Al substitution and 10 Dq are linearly related (top). The increase in 10 Dq can be explained by a decrease of the Fe-(O,OH) bond lengths by 1.2 pm (shown on the right y-axis). The increase of 10 Dq with decreasing UCl_b (bottom) is therefore much smaller than would be inferred from equal Fe-(O,OH) and Al-(O,OH) distances ("calculated").

$UCL_a = 0.46177 - 0.00880x$; $R^2 = 0.69$; n = 53;
Vegard: $UCL_a = 0.46169 - 0.02120x$
$UCL_b = 0.99548 - 0.05204x$; $R^2 = 0.99$; n = 53;
Vegard: $UCL_b = 0.99555 - 0.05300x$
$UCL_c = 0.30238 - 0.017404x$; $R^2 = 0.97$; n = 53;
Vegard: $UCL_c = 0.30245 - 0.01775x$.

UCL_b and UCL_c follow closely the corresponding Vegard lines (hypothetical straight lines between the UCLs of unsubstituted goethite and those of diaspore). The larger deviation between the observed UCL_a and the Vegard line was explained by an average increase of the H-bond lengths due to structural disorder (Schulze and Schwertmann, 1984).

The UCLs derived from XRD constitute average values of a large number of unit cells, each consisting of 12 octahedra. Theoretically, the smaller UCLs of Al-substituted goethite may be realized in two different ways: (1) Average a large number of the smaller $Al(O,OH)_6$ octahedra and the larger $Fe(O,OH)_6$ octahedra, *i.e.*, the octahedra still have the same sizes as in the end-members goethite and diaspore. The linkage of octahedra with such different sizes should give rise to substantial distortions, which could probably be reduced by the formation of AlOOH clusters within the FeOOH structure. (2) Evenly reduce the oxygen distances in the lattice, which would mean, however, that the oxygen cage is too large for Al(III), and too small for Fe(III).

Case (1) would lower the symmetry of the ligand field around Fe(III) and should cause a splitting of bands which was not observed. Case (2), on the other hand, would explain the observed increase of 10 Dq because

$$10\,Dq = \frac{Q\langle r^4\rangle}{R^5_{Fe-(O,OH)}} \qquad (3)$$

with the Fe-(O,OH) distance, $R_{Fe-(O,OH)}$, the radial distance of the 3d orbitals from the nucleus, r, and Q summarizing the potential of the Argon core (Lever, 1984). The validity of this equation derived from ligand field theory was confirmed recently by molecular orbital calculations of the optical spectra of fayalite (Krasovska *et al.*, 1997). A necessary requirement for the application of Equation (3), a constant degree of covalency, is fulfilled (see below). Therefore, we used Equation (3) to calculate the reduction of $R_{Fe-(O,OH)}$ from 10 Dq. Starting from the data for pure goethite: 10 Dq = 15,770 cm^{-1}, r = 64.5 pm, and $R_{Fe-(O,OH)}$ = 202 pm (Forsyth *et al.*, 1968), a Q of 0.30644×10^9 cm^{-1} can be derived. For x = 0.33 and 10 Dq = 16,220 cm^{-1} (Figure 4, top), a $R_{Fe-(O,OH)}$ of 200.9 pm results. That is, $R_{Fe-(O,OH)}$ is reduced by 1.1 pm (−0.5%) according to the band shifts of the reflectance spectra.

In contrast, a linear interpolation between the $R_{Fe-(O,OH)}$ of goethite (202 pm) and that of diaspore (191 pm, Hill, 1979) would give a reduction by 3.7 pm (−1.8%) for x = 0.33 (and consequently a much higher 10 Dq labeled as "calculated" in Figure 4). This result suggests that the $Fe(O,OH)_6$ octahedra are contracted compared to the unsubstituted goethite, but are still larger than the $Al(O,OH)_6$ octahedra. Consequently, the decrease of the unit-cell with increasing x is due to an intermediate-size octahedron between the two cases described above. This result, in combination with the absence of any band splitting which would indicate a decrease in symmetry of the $Fe(O,OH)_6$ ligand field, can be explained by clustering of $Al(O,OH)_6$ octahedra above the statistical average, in agreement with the conclusions from a previous Rietveld study (Hazemann *et al.*, 1991). Both the size of mismatch between diaspore clusters and the goethite structure, and the limited contractibility of the oxygen cage around Fe, could explain the observed miscibility gap between goethite and diaspore.

The energy of $^6A_1 \rightarrow (^4E;^4A_1)$ and $^6A_1 \rightarrow {}^4E(^4D)$ does not depend on 10 Dq. Using the fixed values of B = 628 cm^{-1} and $C = 5.5B$ = 3454 cm^{-1} (see Materials

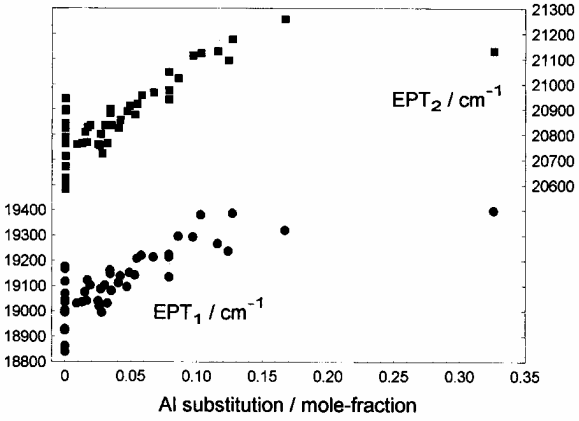

Figure 5. Band shifts of the two electron pair transitions (?) *vs.* Al substitution.

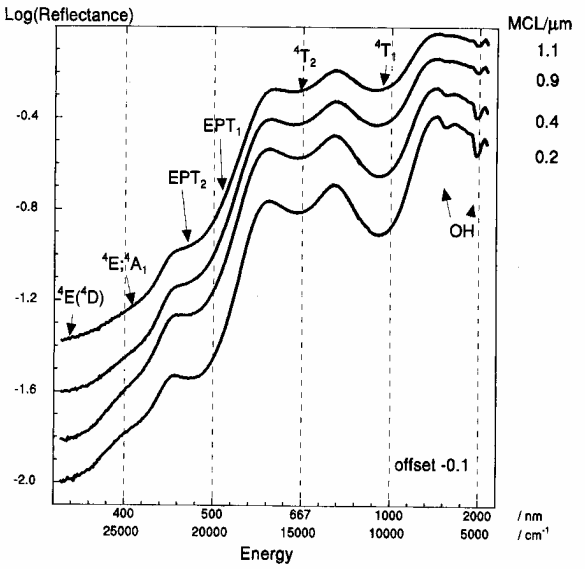

Figure 6. DRS of representative, unsubstituted goethite samples with different mean crystal lengths (MCLs).

and Methods) resulted in constant positions of $^6A_1 \rightarrow (^4E;^4A_1)$ at 23,550 cm^{-1} and of $^6A_1 \rightarrow {}^4E(^4D)$ at 27,950 cm^{-1} in line with the observed spectral features. The invariance of *B* and *C* suggests that the covalency of the Fe-(O,OH) bonds is not influenced by the Al substitution.

The ligand field parameters at $x = 0$ are close to those determined by Sherman and Waite (1985), 10 Dq = 15,320 cm^{-1}, *B* = 590 cm^{-1}, and *C* = 3490 cm^{-1}, although these authors derived the band positions from absorption spectra or from reflectance spectra transformed by the Kubelka-Munk equation. Thus, the different approaches to derive band positions may produce systematic shifts of band positions, but do not influence the derived ligand field parameters.

A spectral feature not predicted by ligand field theory but derived from molecular orbital calculations is the electron pair transition, $(^6A_1 + {}^6A_1 \rightarrow (^4T_1 + {}^4T_1)$, caused by the magnetic coupling of neighboring Fe(III) centers (Schugar *et al.*, 1970; Sherman and Waite, 1985). Whereas the unsubstituted goethite spectra can be satisfactorily fit with one EPT at about 20,200 cm^{-1}, the spectra of Al goethite require the fit of two bands, above and below the single EPT (Figure 1). Attempts to rearrange the band assignment, *e.g.*, by adding $^6A_1 \rightarrow {}^4T_2(^4D)$ to be able to assign $^6A_1 \rightarrow (^4E;^4A_1)$ to the energetically higher of the two EPTs, did not give conclusive results. The likely decrease of the symmetry by increasing Al substitution could possibly split the EPT. Then, however, we would expect the distance between EPT_1 and EPT_2 to increase with increasing Al, which does not happen (Figure 5). The shift of EPT to higher energy when *x* increases is in line with the results of Kosmas *et al.* (1986). As the EPT is based on the $^6A_1 \rightarrow {}^4T_1$ transition, a shift to lower energy would be more consistent. Thus, neither the band splitting nor the shift to higher energy with increasing *x* corroborates the assignment as (double) EPT. As we cannot offer alternative assignments, the name EPT is still used in the following for band 3 and 4.

The variability of the band positions of the unsubstituted goethites is partly determined by the variability of the UCLs (compare Figure 4, top and bottom) which, in turn, are functions of the temperature during crystal growth (Schwertmann *et al.*, 1985). In addition to these band shifts, unsubstituted goethites show a variation in band intensities and widths. Goethites with a lower reflectance have better separated bands of $^6A_1 \rightarrow {}^4T_1$, $^6A_1 \rightarrow {}^4T_2$ and EPT_2 than samples with a higher reflectance (Figure 6). The overall reflectance of the spectra seems to increase with increasing crystal length. This is confirmed by four bands showing increasing intensities when the crystal size decreases (Figure 7). A discussion is given below.

Influence of Al substitution and crystal size on color

Highly-substituted goethites are redder than goethites with low *x* (Figure 8). The correlation between hue and *x* is, however, small ($r = -0.51$) because of the large scattering of the unsubstituted goethites. The red shift with increasing *x* is opposite to the blue shift of the main absorption edge, represented by EPT_1 and EPT_2 (Figure 5). Thus, there are two reasons why Al substitution itself can not be the basic cause for the variation in hue.

Golden (1978), Winter (1979) and Schwertmann (1991) reported a reddening and darkening when crystal size decreased or surface area increased. This is in line with the parabolic decrease of value and hue for MCL <800 nm (Figure 9). Hue and value are closely related ($r = 0.82$). An increase of absorbance with decreasing particle size has been generally observed

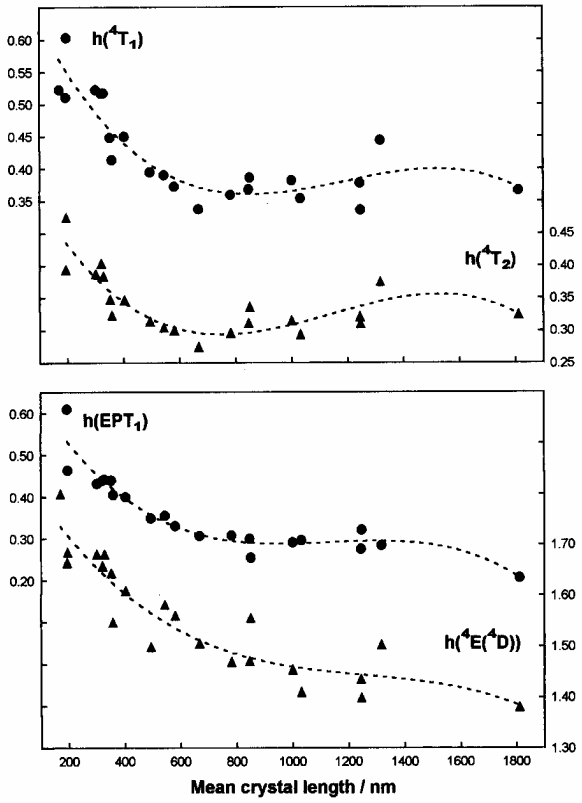

Figure 7. Intensities of the bands $^6A_1 \rightarrow {}^4T_1$, $^6A_1 \rightarrow {}^4T_2$, EPT_1, and $^6A_1 \rightarrow {}^4E(^4D)$ as a function of the mean crystal length.

for strongly absorbing materials (Wendlandt and Hecht, 1966), and it is in line with Mie scattering occurring when the mean diameter of particles is close to the wavelength of the incident light (Mie, 1908; Brockes, 1964; Hapke, 1981; Mustard and Hays, 1997). While the Mie scattering is able to explain the dark shift, there is no easy explanation for the red shift. To investigate the effect of changing reflectance without any changes in band positions, we performed simple manipulations of a typical goethite spectra and calculated the color coordinates. Both a linear decrease of the spectra ($R(E) \rightarrow R(E)$ - a) and a multiplicative decrease ($R(E) \rightarrow R(E) \times$ b, b $<$ 1) to simulate increasing absorption resulted in a shift toward yellow and, thus, opposite to the effect observed on experimental spectra. Using a simplified model from Hapke (1981), Bedidi and Cervelle (1993) found strong, wavelength-dependent oscillations of the absorption and the diffusion efficiency of spherical particles near 200 nm in diameter, whereas both efficiencies were lower and almost wavelength-independent for larger and smaller particles. Due to the sensitivity of color on minute changes of the reflectance curve, this process may lead to the observed changes in color.

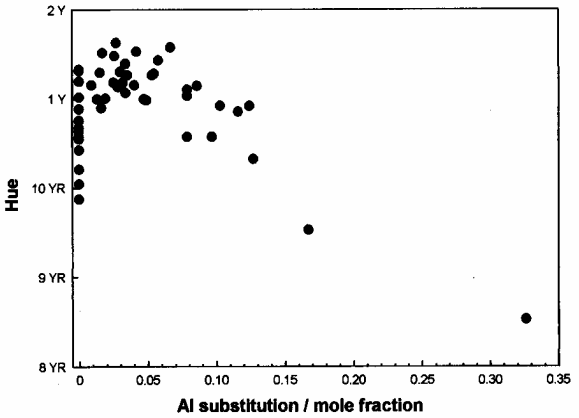

Figure 8. Influence of Al substitution on Munsell hue.

CONCLUSIONS

Spectral and color variations of synthetic goethites were explained by two factors, variation of Fe-(O,OH) distances induced by Al substitution, and variation of crystal size induced by crystal growth temperature or Al substitution. Thus, the smoother shape of the DRS of natural goethite samples (not shown) suggests a broader distribution of Al substitution and crystal size within single samples as compared to the synthetic samples.

Band positions of the spin-forbidden transitions of Fe(III) were reliably extracted from DRS by including the respective ligand field terms into the nonlinear fitting procedure. Due to the improved decomposition method, changes in the Fe-(O,OH) distances of ~0.2 pm could be detected. This is one order of magnitude below the sensitivity limit of Extended X-ray Absorption Fine Structure (EXAFS) spectroscopy (Sayers and Bunker, 1988). Thus, DRS may favorably complement EXAFS studies of transition metal compounds, although it is restricted to information on the first shell (metal-oxygen interaction) (Marco de Lucas *et al.*,

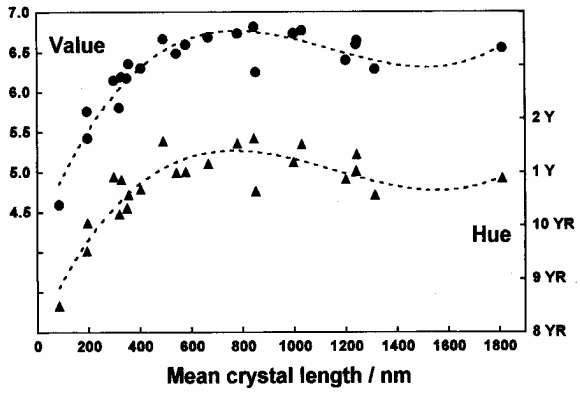

Figure 9. Influence of crystal size on Munsell value and hue.

1995). In spite of the long history of trying to explain d-d transition spectra, starting with the basic work of Bethe (1929), unexplained spectral features still exist.

ACKNOWLEDGMENTS

We thank S. Mansour, Department of Materials Science and Engineering, Purdue University, for providing access to and help with the electron microscope, J. Santini, Department of Agronomy, Purdue University, for her help with SAS, and R. Morris, NASA, Houston Texas, for his helpful review. ACS gratefully acknowledges the support by the Deutsche Forschungsgemeinschaft. This is journal article no. 15889 of the Purdue Agricultural Research Programs.

REFERENCES

Bedidi, A. and Cervelle, B. (1993) Diffusion de la lumière par des particules minérales. *Cahiers ORSTOM Serie Pedologie,* **28,** 7–14.

Bedidi, A., Cervelle, B., Madeira, J., and Pouget, M. (1992) Moisture effects on visible spectral characteristics of lateritic soils. *Soil Science,* **153,** 129–141.

Bethe, H. (1929) Termaufspaltung in Kristallen *Annalen der Physik,* **3,** 133–206.

Bishop, J.L. and Murad, E. (1996) Schwertmannite on Mars? Spectroscopic analyses of schwertmannite, its relationship to other ferric minerals, and its possible presence in the surface material on Mars. In *Mineral Spectroscopy: A Tribute to Roger G. Burns, Special Publication: 5,* M.D. Dyar, C. McCammon, and M.W. Schaefer, eds., The Geochemical Society, Huston, Texas, 400 pp.

Brockes, A. (1964) Der Zusammenhang von Farbstärke und Teichengröße von Buntpigmenten nach der Mie-Theorie. *Optik,* **21,** 550–566.

Buckingham, W.F. and Sommer, S.E. (1983) Mineralogical characterization of rock surfaces formed by hydrothermal alteration and weathering—Application to remote sensing. *Economic Geology,* **78,** 664–674.

Burns, R.G. (1993) *Mineralogical Applications of Crystal Field Theory. Cambridge Topics in Mineral Physics and Chemistry, 5,* A. Putnis and R.C. Lieberman, eds., Cambridge University Press, 551 pp.

Carlson, L. (1995) Aluminum substitution in goethite in lake ore. *Bulletin of the Geological Society of Finland,* **67,** 19–28.

Cornell, R.M. and Schwertmann, U. (1996) *The Iron Oxides: Structure, Properties, Reactions, Occurrence and Uses.* VCH Verlagsgesellschaft, Weinheim, 573 pp.

Fernandez, R.N. and Schulze, D.G. (1987) Calculation of soil color from reflectance spectra. *Soil Science Society of America Journal,* **51,** 1277–1282.

Fitzpatrick, R.W. and Schwertmann, U. (1982) Al-substituted goethite—An indicator of pedogenic and other weathering environments in South Africa. *Geoderma,* **27,** 335–347.

Forsyth, J.B., Hedley, I.G., and Johnson, C.E. (1968) The magnetic structure and hyperfine field of geothite (α-FeOOH). *Journal of Physical Chemistry C Series 2,* **1,** 179–188.

Golden, D.C. (1978) Physical and chemical properties of aluminum-substituted goethite. Dissertation Abstract 7820029, Ph.D. thesis, North Carolina State University.

Hapke, B. (1981) Bidirectional reflectance spectroscopy. 1. Theory. *Journal of Geophysical Research,* **86,** 3039–3054.

Hazemann, J.L., Bérar, J.F., and Manceau, A. (1991) Rietveld studies of the aluminium-iron substition in synthetic goethite. *Materials Science Forum,* **79–82,** 821–825.

Hill, R.J. (1979) Crystal structure refinement and electron density distribution in diaspore. *Physics and Chemistry of Minerals,* **5,** 179–200.

Kosmas, C.S., Curi, N., Bryant, R.B., and Franzmeier, D.P. (1984) Characterization of iron oxide minerals by second-derivative visible spectroscopy. *Soil Science Society of America Journal,* **48,** 401–405.

Kosmas, C.S., Franzmeier, D.P., and Schulze, D.G. (1986) Relationship among derivative spectroscopy, color, crystallite dimensions, and Al substitution of synthetic geothites and hematites. *Clays and Clay Minerals,* **34,** 625–634.

Krasovska, O.V., Winkler, B., Krasovskii, E.E., Yaresko, A.N., Antonov, V.N., and Langer, N. (1997) Ab initio calculation of the pleochroism of fayalite. *American Mineralogist,* **82,** 672–676.

Lever, A.B.P. (1984) *Inorganic Electronic Spectrocopy. Studies in Physical and Theoretical Chemistry,* 33. Elsevier Publishing Company, Amsterdam, 830 pp.

Malengreau, N., Muller, J.-P., and Calas, G. (1994) Fe-speciation in kaolins: A diffuse reflectance study. *Clays and Clay Minerals,* **42,** 137–147.

Malengreau, N., Bedidi, A., Muller, J.-P., and Herbillon, A.J. (1996) Spectroscopic control of iron oxide dissolution in two ferralitic soils. *European Journal of Soil Science,* **47,** 13–20.

Manceau, A. and Combes, J.M. (1988) Structure of Mn and Fe oxides and oxyhydroxides: A topological approach by EXAFS. *Physics and Chemistry of Minerals,* **15,** 283–295.

Marco de Lucas, M.C., Rodríguez, F., Prieto, C., Verdaguer, M., and Güdel, H.U. (1995) Local structure determination of Mn^{2+} in the $ABCl_3$:Mn^{2+} chloroperovskites by EXAFS and by optical spectroscopy. *Journal of Physics and Chemistry of Solids,* **56,** 995–1001.

Marusak, L.A., Messier, R., and White, W.B. (1989) Optical absorption spectrum of hematite, α-Fe_2O_3 near IR to UV. *Journal of Physics and Chemistry of Solids,* **41,** 981–984.

Melville, M.D. and Atkinson, G. (1985) Soil colour: Its measurement and its designation in models of uniform colour space. *Journal of Soil Science,* **36,** 495–512.

Mie, G. (1908) Beiträge zur Optik trüber Medien, speziell kolloidaler Metallösungen. *Annalen der Physik,* **25,** 377–445.

Morris, R.V., Schulze, D.G., Lauer, H.V., Agresti, D.G., and Shelfer, T.D. (1992) Reflectivity (visible and near IR), Mössbauer, static magnetic, and X-ray diffraction properties of Aluminum-substituted hematites. *Journal of Geophysical Research,* **97,** 10257–10266.

Morris, R.V., Golden, D.C., and Bell, J.F., III (1997) Low-temperature reflectivity spectra of red hematite and the color of Mars. *Journal of Geophysical Research,* **102,** 9125–9131.

Mustard, J.F. and Hays, J.E. (1997) Effects of hyperfine particles on relectance spectra from 0.3 to 2.5 μm. *Icarus,* **125,** 145–163.

Orgel, L.E. (1952) The effects of crystal fields on the properties of transition metal ions. *Journal of the Chemical Society,* 4756–4761.

Orgel, L.E. (1957) Ion compresion and the colour of ruby. *Nature,* **179,** 1348.

Reinen, D. (1969) Ligand-field spectroscopy and chemical bonding in Cr^{3+}-containing solids. In *Structure and Bonding 6,* P. Hemmerich, *et al.,* eds., Springer-Verlag, New York, 30–51.

SAS Institute Inc. (1988) *SAS/STAT User's Guide.* Cary, North Carolina, 1028 pp.

Sayers, D.E. and Bunker, B.A. (1988) Data Analysis. In *X-Ray Absorption—Principles, Applications, Techniques of EXAFS, SEXAFS and XANES. Chemical Analysis,* D.C. Koningsberger and R. Prins, eds., John Wiley & Sons, New York, 211–253.

Scheinost, A.C., Chavernas, A., Barrón, V., and Torrent, J. (1998) Use and limitations of second-derivative diffuse re-

flectance spectroscopy in the visible to near-infrared range to identify and quantify Fe oxide minerals in soils. *Clays and Clay Minerals,* **46,** 528–537.

Schugar, H.J., Rossman, G.R., Thibeault, J., and Gray, H.B. (1970) Simultaneous pair electronic excitations in binuclear iron (III) complex. *Chemical Physics Letters,* **6,** 26–28.

Schulze, D.G. (1984) The influence of aluminum on iron oxides. VIII. Unit cell dimensions of Al-substitued geoethites and estimation of Al from them. *Clays and Clay Minerals,* **32,** 36–44.

Schulze, D.G. and Schwertmann, U. (1984) The influence of aluminum on iron oxides: X. Properties of Al-substituted goethites. *Clay Minerals,* **19,** 521–529.

Schulze, D.G. and Schwertmann, U. (1987) The influence of aluminum on iron oxides: XIII. Properties of goethites synthesised in 0.3 M KOH at 25°C. *Clay Minerals,* **22,** 83–92.

Schwertmann, U. (1991) Relations between iron oxides, soil color and soil formation. In *Soil Color,* J.M. Bigham and E.J. Ciolkosz, eds., Soil Science Society of America Special Publication 31, Madison, Wisconsin, 51–69.

Schwertmann, U. and Carlson, L. (1994) Aluminum substitution of iron oxides: XVII. Unit cell parameters and aluminum substitution of natural goethites. *Soil Science Society of America Journal,* **58,** 256–261.

Schwertmann, U., Gasser, U., and Sticher, H. (1989) Chromium-for-iron substitution in synthetic goethites. *Geochimica et Cosmochimica Acta,* **53,** 1293–1297.

Shannon, R.D. (1976) Revised effective ionic radii and systematic studies of interatomic distances in halides and chalcogenides. *Acta Crystallographica,* **A 32,** 751–767.

Sherman, D.M. (1985) Electronic structures of Fe^{3+} coordination sites in iron oxides: applications to spectra, bonding, and magnetism. *Physics and Chemistry of Minerals,* **12,** 161–175.

Sherman, D.M. and Waite, T.D. (1985) Electronic spectra of Fe^{3+} oxides and oxide hydroxides in the near IR to near UV. *American Mineralogist,* **70,** 1262–1269.

Sherman, D.M., Burns, R.G., and Burns, V.M. (1982) Spectral characteristics of the iron oxides with application to the martian bright region mineralogy. *Journal of Geophysical Research,* **87,** 10169–10180.

Singer, R.B. (1982) Spectral evidence for the mineralogy of high-albedo soils and dust on Mars. *Journal of Geophysical Research,* **87,** 10159–10168.

Sunshine, J.M., Pieters, C.M., and Pratt, S.F. (1990) Deconvolution of mineral absorption bands: An improved approach. *Journal of Geophysical Research,* **95,** 6955–6966.

Tossell, J.A. and Vaughan, D.J. (1974) The electronic structure of rutile, wustite, and hematite from molecular orbital calculations. *American Mineralogist,* **59,** 319–334.

Townsend, T.E. (1987) Discrimination of iron alteration minerals in visible and near-infrared reflectance data. *Journal of Geophysical Research,* **92,** 1441–1454.

Wendlandt, W.W. and Hecht, H.G. (1966) *Reflectance Spectroscopy.* John Wiley & Sons, New York, 298 pp.

Winter, G. (1979) Anorganische Pigmente: Disperse Festkörper mit technisch verwertbaren optischen und magnetischen Eigenschaften. *Fortschritte der Mineralogie,* **57,** 172–202.

Wolska, E. and Schwertmann, U. (1993) The mechanism of solid solution formation between goethite and diaspore. *Neues Jahrbuch für Mineralogie Monatshefte,* **5,** 213–223.

Wyszecki, G. and Stiles, W.S. (1982) *Color Science: Concepts and Methods, Quantitative Data and Formulae.* John Wiley and Sons, New York, 950 pp.

(Received 6 January 1998; accepted 6 September 1998; Ms. 98-004)